Spatial regulation of microRNA gene expression in the *Drosophila* embryo

Frédéric Biemar*, Robert Zinzen*, Matthew Ronshaugen*, Victor Sementchenko†, J. Robert Manak†, and Michael S. Levine*‡

*Division of Genetics and Development, Department of Molecular Cell Biology, Center for Integrative Genomics, University of California, Berkeley, CA 94720; and †Affymetrix, Inc., Santa Clara, CA 95051

Contributed by Michael S. Levine, September 8, 2005

MicroRNAs (miRNAs) regulate posttranscriptional gene activity by binding to specific sequences in the 3′ UTRs of target mRNAs. A number of metazoan miRNAs have been shown to exhibit tissue-specific patterns of expression. Here, we investigate the possibility that localized expression is mediated by tissue-specific enhancers, comparable to those seen for protein-coding genes. Two miRNA loci in *Drosophila melanogaster* are investigated, the *mir-309–6* polycistron (8-miR) and the *mir-1* gene. The 8-miR locus contains a cluster of eight distinct miRNAs that are transcribed in a common precursor RNA. The 8-miR primary transcript displays a dynamic pattern of expression in early embryos, including repression at the anterior and posterior poles. An 800-bp 5′ enhancer was identified that recapitulates this complex pattern when attached to a RNA polymerase II core promoter fused to a *lacZ*-reporter gene. The miR-1 locus is specifically expressed in the mesoderm of gastrulating embryos. Bioinformatics methods were used to identify a mesoderm-specific enhancer located ≈5 kb 5′ of the miR-1 transcription unit. Evidence is presented that the 8-miR enhancer is regulated by the localized Huckebein repressor, whereas miR-1 is activated by Dorsal and Twist. These results provide evidence that restricted activities of the 8-miR and miR-1 miRNAs are mediated by classical tissue-specific enhancers.

development | enhancer | transcription

MicroRNAs (miRNAs) are short, 18- to 24-nt-long noncoding RNAs that mediate posttranscriptional gene silencing by annealing to complementary sequences in the 3′ UTRs of target mRNAs. This type of regulation modulates gene expression through the inhibition of protein synthesis and/or mRNA stability (1–3). A variety of experimental and computational studies have characterized miRNA biogenesis and miRNA–mRNA interactions (4–6). In addition, the function of an increasing number of miRNAs has been described (7, 8). However, considerably less is known about the regulation of miRNA gene expression, despite the fact that many miRNAs display tissue-specific patterns of gene expression during embryogenesis.

There is evidence that miRNAs are transcribed as large (>1 kb) nuclear precursor RNAs, which are subsequently processed into definitive miRNAs (9). The primary transcripts appear to be produced from RNA polymerase II (pol II) core promoters, but there is very little information about the basis for localized patterns of miRNA gene activity (10, 11). In particular, does the differential processing of ubiquitous precursor RNAs produce spatially localized miRNAs, or do cell-specific enhancers, comparable to those seen for protein-coding genes, generate them?

The analysis of one of the prototypic miRNA genes, *let-7* in *Caenorhabditis elegans*, led to the identification of an enhancer that is responsible for its temporal pattern of expression (12). There is a sharp increase in the levels of let-7 expression in late larval and adult stages. The enhancer is located 1.2 kb 5′ of the mature let-7 miRNA and recapitulates the normal temporal expression profile when attached to a GFP-reporter gene and assayed in transgenic animals. Another recent study (13) has identified a 5′ enhancer that directs miR-1 expression in cardiac and skeletal muscle precursors in the mouse embryo. This enhancer appears to be activated by known sequence-specific transcription factors, including serum response factor (SRF) and MyoD.

Here, we investigate the possibility that spatially localized miRNAs are regulated by cell-specific enhancers in the *Drosophila* embryo. The miR-309-6 cluster (referred to here as "8-miR") in *Drosophila* encodes eight distinct miRNAs: miR-309, miR-3, miR-286, miR-4, miR-5, miR-6–1, miR-6–2, and miR-6–3. All eight miRNAs are likely processed from a single ≈1.5-kb primary transcript, which displays a dynamic pattern of expression in the early embryo. An 800-bp enhancer is identified that directs the salient features of the 8-miR expression profile when attached to a *lacZ*-reporter gene. Similarly, the *Drosophila miR-1* gene displays localized expression in the mesoderm of gastrulating embryos. The FLYENHANCER program (14) identified a cluster of Dorsal- and Twist-binding sites located ≈5 kb upstream of the putative miR-1 transcription start site. An ≈1-kb genomic DNA fragment encompassing these binding sites mediates localized expression of a *lacZ*-reporter gene in the mesoderm of transgenic embryos. These results suggest that miR-1 is a legitimate and direct component of the Dorsal genomic regulatory network governing gastrulation. We conclude that cell-specific enhancers, comparable to those seen for protein-coding genes, regulate spatially localized patterns of miRNA gene expression.

Materials and Methods

Fly Strains and Generation of Transgenic Lines. The tor^{D}, hkb^{2}, tll^{L10}, $pipe^{386}/pipe^{664}$, $Toll^{rm9}/Toll^{rm10}$, $Toll^{10B}$, $snail^{IIG}$, $twist^{ID96}$, and $twist^{IIH};snail^{IIG}$ double-mutant stocks were used. WT embryos were obtained from the yw^{67} *Drosophila melanogaster* strain. For the 8-miR enhancer, an 800-bp fragment, containing the entire genomic region between miR-3 and the predicted start site of CG11018, was amplified with the following primers: fb98, 5′-GTGAGATTGAAACATAACTGCA-3′, and fb99, 5′-CTTCGATTGCTAACTAGGCC-3′. The miR-1 enhancer was identified by using FLYENHANCER (www.flyenhancer.org; ref. 14) based on clustering of transcription factor-binding sites, particularly Dorsal and Twist sites. A 1,169-bp fragment was PCR-amplified by using the following primers: RZ-F111b, 5′-GTCTTAGGGATGGGGATTTCAGGGG-3′, and RZ-R111, 5′-CAATGATTATGGTTCCGCCG-3′. The PCR products were cloned into pGem T-Easy vector (Promega), subcloned into the P-element vector pE2G (15) with NotI, and verified for identity and orientation by sequencing. P-element-mediated transformation was performed with standard methods (16). Several independent lines were tested for each construct.

Abbreviations: Hkb, Huckebein; miRNA, microRNA; Htl, Heartless.

‡To whom correspondence should be addressed. E-mail: mlevine@berkeley.edu.

***In Situ* Hybridization and Microscopy.** Embryos were collected, fixed, and then hybridized with dioxygenin-UTP or biotin-UTP-labeled antisense riboprobes as described (17). Templates for the *pri-mir-309-6* and *pri-mir-1* probes were obtained by using oligonucleotide primers in PCR on genomic DNA obtained from WT flies, using the following primers: fb157, 5′-CCCAAATGTTCAAAGCTTGAG-3′, and fb160, 5′-CCGATCCTGGGATGCATCT-3′, for *pri-mir-309-6*; and fb181, 5′-CCGAAAAGCAGAAACAAAGC, and fb182, 5′-CGAATGTTTGTTGTCGATGG-3′, for *pri-mir-1*. The *sna* and *lacZ* probes have been described (18). The following primary Abs were used: sheep anti-digoxigenin (1:400; Roche Biochemicals) and mouse anti-BIO (1:400; Roche Biochemicals). Alexa Fluor 488 donkey anti-sheep (1:400; Molecular Probes) and Alexa Fluor 555 donkey anti-mouse (1:400; Molecular Probes) were used to detect the primary Abs. The samples were mounted in VECTASHIELD with DAPI (Vector Laboratories), and FISH images were obtained with a Leica LS confocal microscope.

The 5′ RACE Assays. For 5′ RACE experiments, poly(A)$^+$ RNA was isolated from WT embryos, aged 0–6 and 6–12 h, with a Oligotex kit (Qiagen, Valencia, CA). cDNA template was obtained by using the Marathon cDNA amplification kit (Clontech). The following gene-specific primers were used: fb161, 5′-AGATGCATCCCAGGATCGGGACC-3′, and fb162, 5′-CTGGCTTGGAAATTGGCAAAACCG-3′.

Whole-Genome Tiling Arrays. Total RNA was extracted from *pipe^{386}/pipe^{664}*, *Toll^{rm9}/Toll^{rm10}*, and *Toll^{10B}* mutant embryos as described (19). First-strand cDNA synthesis was performed by using SuperScript II reverse transcriptase in the reaction volume of 105 μl for 15 μg of starting RNA material. The RNA was mixed with random hexamers (83.3 ng/g mRNA), heated to 70°C for 10 min, and cooled to 15°C after which 5× SuperScript II First Strand buffer, DTT (10 mM), and dNTPs (0.5 mM) were added. SuperScript II was added after a 20-min incubation (200 units/μg RNA) followed by a 20-min ramp to 42°C and 60-min incubation at 42°C. SuperScript II was inactivated at 75°C for 15 min. The second-strand cDNA was synthesized by addition of 50 units of *Escherichia coli* DNA ligase, 200 units of *E. coli* DNA polymerase I, 10 units of *E. coli* RNase H, and 0.2 mM dNTPs to the first-strand synthesis reaction at 16°C for 2 h. Double-stranded cDNA was treated with RNase H (Epicentre Technologies, Madison, WI) and RNases A/T1 (Ambion, Austin, TX), extracted by using a QIAquick PCR purification kit (Qiagen), and subjected to further fragmentation to 50–100 bp by DNase I (1 unit/μl; Epicentre Technologies; size distribution of fragmented DNA was verified on a 2% agarose gel). The fragmented cDNA was then end-labeled with 70 nM bio-dideoxy ATP (PerkinElmer) by using 6–10 units of terminal deoxynucleotidyltransferase (Roche Diagnostics) per μg of fragmented DNA in 1× TdT buffer (Roche Diagnostics) and 5 mM $CoCl_2$ (Roche Diagnostics) for 2 h at 37°C. The labeled DNA material was subsequently hybridized to Affymetrix *Drosophila*-tiled genomic microarrays for 18 h at 45°C in a 3 M tetramethyl ammonium chlorate/1× Mes-based solution. All reagents were from Invitrogen, except where noted otherwise.

The signal is an estimate of RNA abundance by using a Wilcoxon sign rank scan statistic where the median of all pairwise average values of perfect match probe signal minus mismatch probe signal is calculated for all probe pairs within a sliding window of 101 bp of chromosomal position by using quantile normalizing replicate arrays whose median array intensity was scaled to 25.

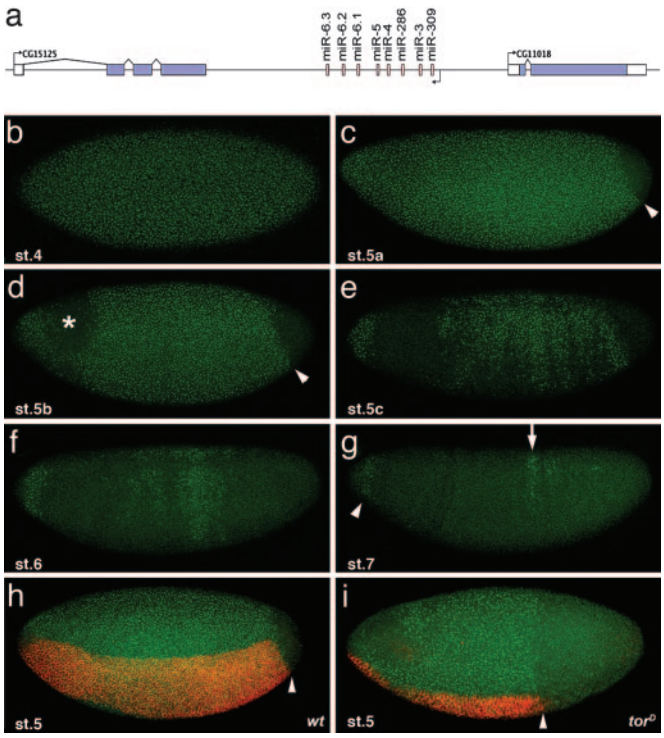

Fig. 1. Expression pattern of the 8-miR primary transcript in WT and mutant embryos. All embryos are oriented to show lateral views with anterior to the left and dorsal to the top. (*a*) Diagram representing the intergenic region containing the 8-miR locus, between CG15125 and CG11018. Direction of transcription is indicated by arrows. (*b*) Precellular embryo, stage 4, showing ubiquitous expression. (*c–e*) Stage 5 embryos showing the repression at the posterior pole (arrowhead) and anterior region (asterisk). (*f* and *g*) During gastrulation, stages 6 and 7, the 8-miR transcripts are progressively restricted to stripes in the dorsal ectoderm. (*h* and *i*) Double labeling experiments showing expression of the 8-miR (green) and *snail* (red) transcripts in stage 5, WT (*h*) and *tor^D* mutant (*i*) embryos. The arrowhead indicates the posterior border of expression. Schematics in Figs. 1 and 4 were obtained by using GENEPALETTE software developed by Mark Rebeiz and Jim Posakony (www.genepalette.org).

Results and Discussion

The 8-miR complex is located between two predicted protein-coding genes, CG15125 and CG11018, in the 56E region on the right arm of chromosome 2 (Fig. 1*a*). To determine the approximate transcription start site of the 8-miR transcription unit, 5′ RACE was used. Several independent experiments were carried out, and RACE products corresponding to two different start sites were isolated several times. Consensus sequences for both an initiator and a TATA box are appropriately spaced upstream of the identified start sites. The alignment of this genomic interval with the corresponding regions of the most divergent Drosophilids indicates strong conservation of each of the individual miRNAs within the 8-miR complex (data not shown).

A digoxigenin-labeled 8-miR antisense RNA probe was hybridized to staged embryos to determine the expression profile of the precursor transcript during development (Fig. 1 *b–g*). Expression is initially detected in all of the nuclei of precellular embryos. As expected, staining is restricted to nuclei and not seen in the cytoplasm (e.g., Fig. 1*b*). The first indication of differential spatial regulation occurs at the midpoint of cellularization, when 8-miR transcripts are lost at the posterior pole (Fig. 1*c*, arrowhead). By the completion of cellularization, this loss in staining expands and there is also reduced expression in anterior regions (Fig. 1*d*, asterisk). Staining persists at the

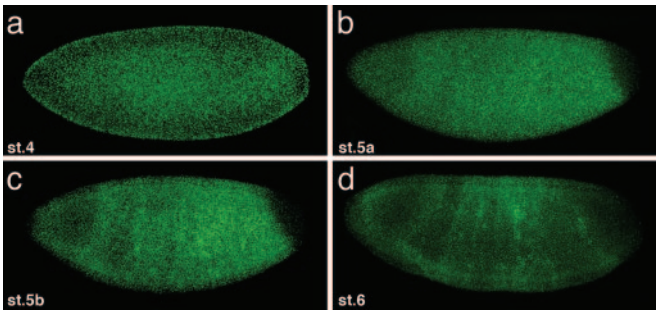

Fig. 2. The 8-miR enhancer recapitulates the endogenous expression pattern. Transgenic flies expressing *eve-lacZ* under the control of an 800-bp upstream region exhibit the same posterior and then dorso-ventral repression as the endogenous transcript. Note that *lacZ* transcripts are observed strictly in the cytoplasm. The numbers in the lower left corners indicate the embryonic stage.

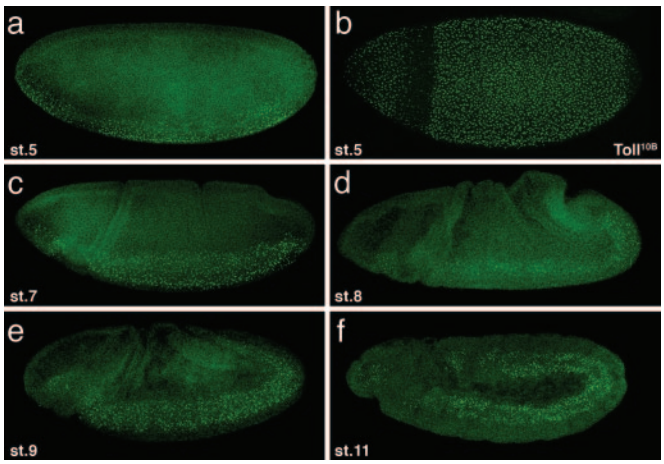

Fig. 3. Expression pattern of the *mir-1* primary transcript in WT and mutant embryos. Embryos are oriented to show lateral views with anterior to the left and dorsal up. (*a* and *b*) Localization of *mir-1* primary transcripts in the mesoderm of a stage 5 WT (*a*) and $Toll^{10B}$ mutant (*b*) embryo. (*c–f*) Progressively older WT embryos show faithful expression of miR-1 expression in the mesoderm. The numbers in the lower left corners indicate the embryonic stage.

anterior tip but is lost from subterminal regions of the anterior pole (Fig. 1*e*).

During gastrulation there is both dorsal-ventral and anterior-posterior modulation of the 8-miR-staining pattern (Fig. 1 *f* and *g*). Staining is first lost from the presumptive mesoderm and neurogenic ectoderm in ventral and lateral regions. There are transient stripes of 8-miR expression in the dorsal ectoderm (Fig. 1*e*), but they rapidly give way to a single band of staining in central regions (Fig. 1*f*). By the onset of the rapid phase of germband elongation, staining is essentially lost except for residual expression at the anterior tip and dorsal ectoderm (Fig. 1*g*, arrow).

The early loss of staining at the posterior pole suggests that Huckebein (Hkb) might repress 8-miR transcription in the early embryo. To investigate this possibility, colocalization assays were done with *snail*, which is selectively expressed in the presumptive mesoderm of cellularizing and gastrulating embryos (Fig. 1*h* and ref. 20). The posterior border of the *snail* pattern is established by the localized Hkb repressor. The 8-miR pattern displays a similar posterior border (Fig. 1*h*, arrowhead), and there is an expansion of both the *snail* and 8-miR patterns in hkb^{-}/hkb^{-} mutant embryos (data not shown).

Further evidence for repression by Hkb was obtained by analyzing *torso* dominant (tor^{D}) mutants (Fig. 1*i*). *tor* encodes a receptor tyrosine kinase that is normally activated only at the poles, where it is required for the localized expression of *tailless* (*tll*) and *hkb* (21). tor^{D} encodes a constitutively activated form of the receptor tyrosine kinase that results in expanded expression of *hkb* and *tll* at the poles. This expansion in Hkb causes a severe shift in the posterior border of both the *snail* and 8-miR expression patterns (Fig. 1*i*, arrowhead). The identification of a sequence-specific transcriptional repressor, Hkb, as a likely regulator of 8-miR expression suggests that the dynamic staining pattern is probably controlled at the level of *de novo* transcription.

Direct support for this possibility was obtained by the identification of an 8-miR enhancer. An ≈800-bp genomic DNA fragment extending from the miR-3 region of the 8-miR complex to the predicted start site of CG11018 was attached to a *lacZ*-reporter gene containing the minimal *eve* promoter sequence. The resulting fusion gene recapitulates most aspects of the endogenous 8-miR expression pattern (Fig. 2 *a–d*; compare with Fig. 1 *b–f*). In particular, *lacZ* transcripts are initially detected throughout precellular embryos (Fig. 2*a*) but sequentially lost from the posterior pole (Fig. 2*b*) and anterior regions (Fig. 2*c*) during cellularization. At the onset of gastrulation, expression is diminished in ventral regions, and the staining detected in the dorsal ectoderm exhibits segmental modulation (Fig. 2*d*). Thus, the 5′ 8-miR enhancer contains repression elements that mediate silencing by Hkb (and possibly Tll) at the termini in response to Tor signaling.

The preceding analysis provides evidence that cell-specific enhancers regulate miRNA gene expression, as seen for protein coding genes. Further support was obtained by analyzing a second miRNA that displays localized expression in the early *Drosophila* embryo, miR-1 (Fig. 3). The *mir-1* gene is highly conserved in different animal groups and displays localized expression in a variety of mesodermal lineages, including cardiac mesoderm in vertebrates (e.g., refs. 13 and 22). The *Drosophila mir-1* gene is first expressed in the presumptive mesoderm during the final phases of cellularization (Fig. 3*a*). Expression persists in differentiating mesodermal tissues during gastrulation, germband elongation, and segmentation (Fig. 3 *c–f*). Mutant embryos that contain the constitutively activated $Toll^{10B}$ receptor display ubiquitous expression of miR-1, concomitant with the transformation of all of the tissues into mesoderm (Fig. 3*b*).

Whole-genome tiling arrays were used to obtain an estimate of the miR-1 transcription unit (Fig. 4*a*). These high-density oligonucleotide arrays contain 25-nt oligomers spaced on average every 36 bp and cover the entire nonrepetitive *Drosophila* genome, from one end of each chromosome to the other. Total RNA was extracted from three different mutant strains. Embryos derived from $pipe^{-}/pipe^{-}$ females lack Toll-signaling activity and thereby lack a Dorsal nuclear gradient. As a result, genes normally activated by high, intermediate, and low levels of the gradient are silent, and there is a loss of mesoderm and neurogenic ectoderm. Instead, genes that are repressed by the Dorsal gradient, and normally restricted to the dorsal ectoderm, are now expressed throughout the embryo, causing the transformation of mesoderm and neurogenic ectoderm into dorsal ectoderm. Previous microarray assays have shown that genes expressed in the dorsal ectoderm are overexpressed in mutant embryos derived from $pipe^{-}/pipe^{-}$ embryos (19). As expected, such mutants display little or no expression of the miR-1 transcription unit (Fig. 4*a*). Similarly, embryos derived from $Toll^{rm9}/Toll^{rm10}$ mutants contain weak Toll signaling and low levels of nuclear Dorsal everywhere. These low levels are insufficient for the activation of mesoderm genes, but are sufficient for the activation of neurogenic genes and the repres-

DEVELOPMENTAL BIOLOGY

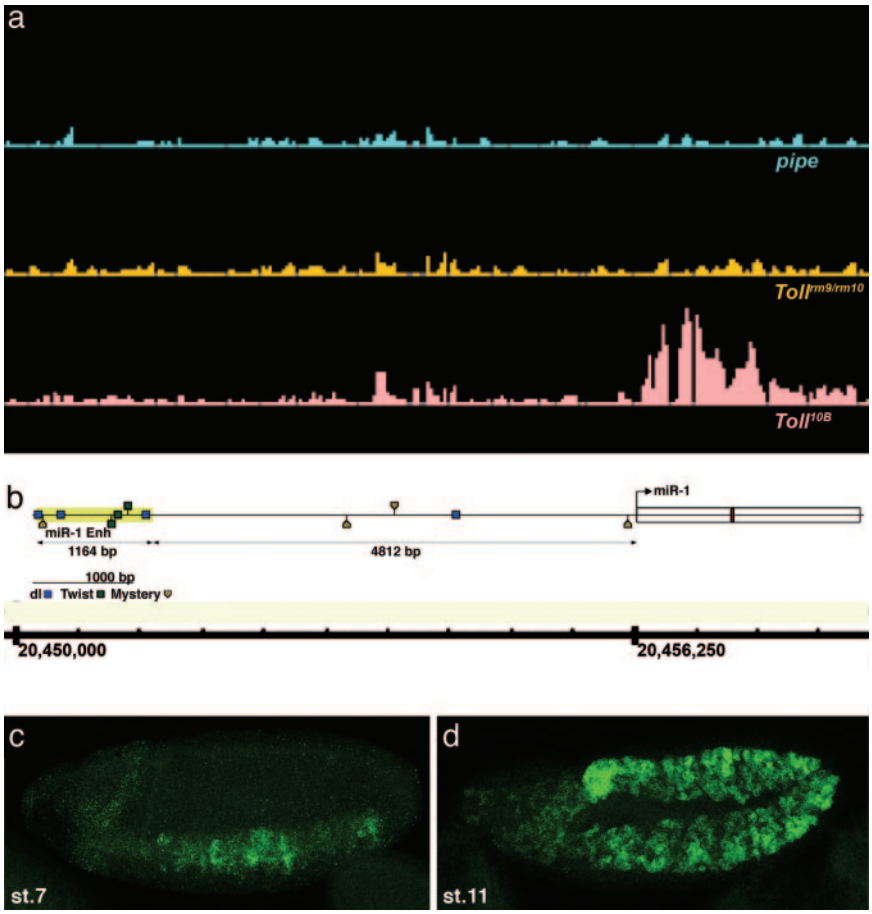

Fig. 4. Identification of the *mir-1* primary transcript and upstream enhancer. (*a*) Graphs of transcription activity in an ≈8-kb window surrounding the miR-1 locus. The blue graph represents total cellular transcripts from $pipe^{-}/pipe^{-}$ mutants; the orange graph represents transcripts from $Toll^{rm9}/Toll^{rm10}$ mutant embryos, and the pink graph represents *mir-1* primary transcripts in $Toll^{10B}$ mutant embryos. (*b*) The tiling arrays predict an ≈2.2-kb primary transcript and bioinformatics identify an enhancer ≈5-kb upstream of the predicted transcription start site. (*c* and *d*) Transgenic flies expressing *eve-lacZ* under the control of the predicted enhancer recapitulate the late mesoderm-specific endogenous pattern. Both embryos are in lateral views, with anterior to the left and dorsal to the top.

sion of dorsal ectoderm genes. Again, these mutants fail to express miR-1 (Fig. 4*a*). $Toll^{10B}$ embryos contain strong, ubiquitous Toll signaling and high levels of Dorsal, which activate mesoderm genes throughout the embryo. These embryos display strong expression of the miR-1 transcription unit. The tiling array suggests that the gene is ≈2.9 kb in length. The mature, processed miRNA is located roughly in the center of the inferred transcription unit (Fig. 4*b*).

The early expression of the miR-1 primary transcript in the mesoderm raises the possibility that the gene might be regulated by the Dorsal gradient. Approximately one-half of all Dorsal-target enhancers also contain binding sites for the basic helix–loop–helix Twist activator. A 50-kb interval encompassing the miR-1 locus was surveyed for clusters of Dorsal and Twist binding sites. The best cluster was identified ≈5 kb upstream of the miR-1 start site (Fig. 4*b*). There are a total of three Dorsal- and four Twist-binding sites contained over an interval of ≈1.1 kb in this distal 5′ region.

A genomic DNA fragment encompassing these sites was attached to a *lacZ*-reporter gene and expressed in transgenic embryos (Fig. 4 *c* and *d*). The reporter gene exhibits localized expression in the ventral mesoderm, beginning at the onset of gastrulation (Fig. 4*c*). Expression persists during germband elongation (Fig. 4*d*). These observations suggest that miR-1 is directly activated by Dorsal and Twist. However, *lacZ* transcripts expressed from the miR-1::lacZ transgene are detected somewhat later than the endogenous miR-1 primary transcript, which first appears before the completion of cellularization. It is conceivable that the miR-1 locus contains a second enhancer that directs earlier expression.

The preceding analysis provides evidence that dynamic patterns of miRNA gene expression are controlled by tissue-specific enhancers, and not by the differential processing of miRNA precursor RNAs. Both the 8-miR and miR-1 enhancers produce authentic patterns of *lacZ*-reporter gene expression when attached to the core promoter region of the *eve* gene. The 8-miR enhancer appears to be regulated by the Hkb repressor, whereas miR-1 is activated by Dorsal and Twist.

The miR-1 enhancer is somewhat unusual among "type 1" Dorsal target enhancers, in that it contains a large number of Snail repressor sites. Type 1 enhancers are activated by high levels of the Dorsal gradient in the ventral mesoderm (reviewed in ref. 23). Previous studies have identified six such enhancers. They all contain multiple low-affinity Dorsal binding sites, but essentially lack Snail repressor sites. The general absence of Snail sites permits activation of type 1 genes in the ventral mesoderm where there are high levels of the repressor. An exception is the type 1 intronic enhancer that regulates Heartless (Htl), one of the two FGF receptor genes in the *Drosophila* genome.

The *htl* intronic enhancer is ≈800 bp in length and contains two low-affinity Dorsal binding sites and two optimal Twist sites

(24). Each Twist site overlaps a Snail repressor site, but the enhancer nonetheless activates *lacZ*-reporter gene expression in the presumptive mesoderm before the completion of cellularization. The *htl* enhancer fails to mediate expression in the neurogenic ectoderm because it lacks the arrangement of optimal Dorsal and Twist sites required for activation by intermediate levels of the Dorsal gradient (type 2 enhancers).

The miR-1 enhancer contains three weak Dorsal sites, four optimal Twist sites (CACATGT; Kate Senger, unpublished results), and five Snail repressor sites (three of the sites overlap the optimal Twist sites and two occur at separate sites). Perhaps the relative increase in the number of Snail repressor sites in the miR-1 enhancer (vs. the *htl* enhancer) causes late onset of miR-1::lacZ transgene expression. The Snail repressor is transiently expressed in the ventral mesoderm during cellularization but disappears after invagination. It is during the time when Snail levels subside that the miR-1 enhancer first becomes active.

Previous studies have emphasized the importance of the Snail repressor in defining spatially localized patterns of gene expression. Dorsal target genes activated by intermediate (type 2) and low (type 3) levels of the gradient contain Snail repressor sites that keep the genes off in the ventral mesoderm and restricted to the neurogenic ectoderm. The present identification of the distal miR-1 enhancer raises the possibility that Snail also influences the timing of gene expression.

The similarities in miR-1 and Htl regulation raise the possibility that the miR-1 miRNA attenuates the activity of one or more components of the FGF-signaling pathway. FGF is essential for the migration of the invaginated mesoderm along the inner surface of the neurogenic ectoderm (reviewed in ref. 25). It is also important for the activation of cardiac genes in the dorsal-most mesoderm that forms the heart (reviewed in ref. 26). miR-1 might attenuate one or more target mRNAs engaged in mesoderm migration and/or heart induction. The mammalian miR-1 miRNA has been shown to attenuate Hnd2 expression, which is essential for the differentiation of ventricular cardiomyocytes (13). Despite the conservation of the miR-1 miRNA sequence, and a potential role in suppressing heart formation in both flies and mice, it would appear that distinct mechanisms of regulation are used in the two systems: Dorsal and Twist activate miR-1 in flies, whereas distinct regulatory factors, SRF and MyoD, activate miR-1 in the mouse embryo. It is possible however, that later phases of miR-1 expression depend on *nautilus* (*nau*), the *Drosophila* homolog of MyoD (27).

We thank Jessica Piel and Ian Bell for excellent technical assistance; Pavel Tomancak, Eric Lai, and Aziz Aboobaker for helpful discussion and for sharing unpublished results; and Michele Markstein for insightful comments on the manuscript. This work was funded by National Institutes of Health Grant GM34431.

1. Lai, E. C. (2003) *Curr. Biol.* **13,** R925–R936.
2. Bartel, D. P. & Chen, C. Z. (2004) *Nat. Rev. Genet.* **5,** 396–400.
3. Bagga, S., Bracht, J., Hunter, S., Massirer, K., Holtz, J., Eachus, R. & Pasquinelli, A. E. (2005) *Cell* **122,** 553–563.
4. Vella, M. C., Reinert, K. & Slack, F. J. (2004) *Chem. Biol.* **11,** 1619–1623.
5. Brennecke, J., Stark, A., Russell, R. B. & Cohen, S. M. (2005) *PLoS Biol.* **3,** e85.
6. Kim, V. N. (2005) *Nat. Rev. Mol. Cell Biol.* **6,** 376–385.
7. Ambros, V. (2004) *Nature* **431,** 350–355.
8. Pasquinelli, A. E., Hunter, S. & Bracht, J. (2005) *Curr. Opin. Genet. Dev.* **15,** 200–205.
9. Lee, Y., Jeon, K., Lee, J. T., Kim, S. & Kim, V. N. (2002) *EMBO J.* **21,** 4663–4670.
10. Lee, Y., Kim, M., Han, J., Yeom, K. H., Lee, S., Baek, S. H. & Kim, V. N. (2004) *EMBO J.* **23,** 4051–4060.
11. Cai, X., Hagedorn, C. H. & Cullen, B. R. (2004) *RNA* **10,** 1957–1966.
12. Johnson, S. M., Lin, S. Y. & Slack, F. J. (2003) *Dev. Biol.* **259,** 364–379.
13. Zhao, Y., Samal, E. & Srivastava, D. (2005) *Nature* **436,** 214–220.
14. Markstein, M., Markstein, P., Markstein, V. & Levine, M. S. (2002) *Proc. Natl. Acad. Sci. USA* **99,** 763–768.
15. Markstein, M., Zinzen, R., Markstein, P., Yee, K. P., Erives, A., Stathopoulos, A. & Levine, M. (2004) *Development (Cambridge, U.K.)* **131,** 2387–2394.
16. Rubin, G. M. & Spradling, A. C. (1982) *Science* **218,** 348–353.
17. Kosman, D., Mizutani, C. M., Lemons, D., Cox, W. G., McGinnis, W. & Bier, E. (2004) *Science* **305,** 846.
18. Jiang, J., Kosman, D., Ip, Y. T. & Levine, M. (1991) *Genes Dev.* **5,** 1881–1891.
19. Stathopoulos, A., Van Drenth, M., Erives, A., Markstein, M. & Levine, M. (2002) *Cell* **111,** 687–701.
20. Reuter, R. & Leptin, M. (1994) *Development (Cambridge, U.K.)* **120,** 1137–1150.
21. Klingler, M., Erdelyi, M., Szabad, J. & Nusslein-Volhard, C. (1988) *Nature* **335,** 275–277.
22. Mansfield, J. H., Harfe, B. D., Nissen, R., Obenauer, J., Srineel, J., Chaudhuri, A., Farzan-Kashani, R., Zuker, M., Pasquinelli, A. E., Ruvkun, G., *et al.* (2004) *Nat. Genet.* **36,** 1079–1083.
23. Stathopoulos, A. & Levine, M. (2004) *Curr. Opin. Genet. Dev.* **14,** 477–484.
24. Stathopoulos, A., Tam, B., Ronshaugen, M., Frasch, M. & Levine, M. (2004) *Genes Dev.* **18,** 687–699.
25. Leptin, M. & Affolter, M. (2004) *Curr. Biol.* **14,** R480–R482.
26. Fossett, N. & Schulz, R. A. (2001) *Trends Cardiovasc. Med.* **11,** 185–190.
27. Michelson, A. M., Abmayr, S. M., Bate, M., Arias, A. M. & Maniatis, T. (1990) *Genes Dev.* **4,** 2086–2097.